ORIGINAL PAPER

Heterojunction CuO thin coated CaO drived from eggshell waste for fast removal of organic pollutants from water under visible light

A. Ali Ahmed[1,2] · Z. Hattab[2] · Y. Berredjem[2] · A. Giordana[3] · G. Cerrato[3] · R. Djellabi[4]

Abstract

The conversion of food and agro-industrial wastes to produce useful products is one of the goals of economic and sustainable development, as also evidenced in the 2030 Agenda for Sustainable Development, adopted by all United Nations Member States in 2015. This work aims to study the transformation of $CaCO_3$ based eggshell waste (ES) into a face centered cubic oxide form (namely, CaO), followed by CuO coating to be used as photocatalytic material (ES@CuO) for fast removal of basic fuchsin (BF) dye from water under visible light. Different ES@CuO samples with different CuO amounts (2.5, 5 and 10%, respectively) and calcined at different temperatures (600, 800, and 1000 °C) were prepared by hydrothermal method. Samples with CuO from medium to high amounts (5 and 10%) demonstrated excellent photocatalytic activity, as compared to low CuO amount (2.5%). In addition, the samples calcined at higher temperature (800 and 1000 °C) exhibited superior degradation rates, reaching 88.11% and 88.33%, respectively. The effect of operating parameters was investigated to understand the behavior of ES@CuO under different conditions. ES@CuO shows rapid removal of BF which combines adsorption and photooxidation, wherein the removal rate reaches up 99% for a BF dye concentration of 100 ppm within 30 min using 75 mg/L of ES@CuO$_{5\%}$. ES@CuO exhibits superior adsorption ability and excellent photoproduced charges transfer which provide synergistic effects to boost the quick removal of dye from water. The finding of this investigation encourages valorizing food wastes into sustainable materials for water remediation.

Graphical abstract
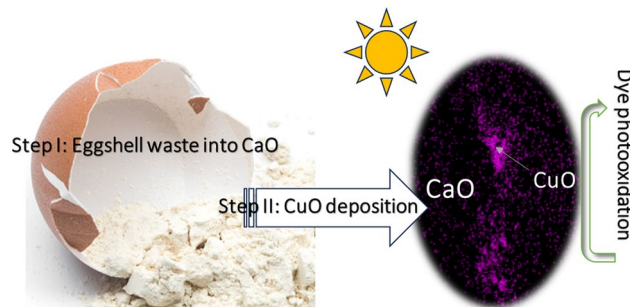
Editorial responsibility: Fatih ŞEN.

Extended author information available on the last page of the article

Introduction

Over the recent decades, punctual environmental, energy and economic restrictions have been launched to reach the goals of sustainable development (Djellabi et al. 2022). The valorization of wastes into high value production and

🙂 Springer

useful materials is one of the promising strategies which has received a lot of attention from both scientific and industrial communities (Ambaye et al. 2023; Galloni et al. 2024). The conversion of wastes into useful products reduces the content of solid wastes in our environment and meanwhile it opens alternative clean and economic produce sources (Aboagye et al. 2023; Andhalkar et al. 2023). Food biowastes are widely available with huge quantities especially in large population cities. Its valorization into different useful materials is very highly recommended from environmental and economic points of view (Nayak and Bhushan 2019). Eggs are an essential and globally consumed food for household and industrial applications. It offers several health benefits, including supporting the healing of body tissues and maintaining a healthy immune system. About 8 million tons of eggshell wastes are globally produced each year, and thrown away as garbage in landfills, becoming a source of a serious environmental issue (De Angelis et al. 2017). Eggshells (ES) represent an abundant source of calcium carbonate and exhibits large number of high value products such as bioactive elements and minerals with high commercial interest (Zaman et al. 2018). Several research studies have been reported to extract natural calcium from eggshells to fortify foods and manufacture vitamins and dietary supplements (Waheed et al. 2019; Singh et al. 2021).

Within the context of biomass valorization, many studies have examined the possible use of eggshell biowaste as a catalyst or/and material in different applications, such as metal matrix composites (Vickers 2017; Ononiwu and Akinlabi 2020), bioactive compounds in anaerobic fermentation (Luo et al. 2020), and even in water treatment (Carvalho et al. 2011; Laca et al. 2017). Li et al. (Mandado et al. 2006) previously demonstrated the effective adsorption of reactive dyes on eggshell based adsorbents. In another study reported by Zhai et al. (2022), $CaCO_3$-containing material generated from eggshell exhibits excellent adsorption ability for dye removal from water. Modified eggshell composites have been widely reported for adsorption or/and (photo)-catalytic applications. Dickon et al. created an eggshell/$MgFe_2O_4$ matrix structure allowing the removal of the antibiotic doxycycline from polluted waters (Li et al. 2017). Other researchers have used eggshells to develop membranes for wastewater treatment, serving as both auxiliary and primary material for photocatalytic degradation (Cao et al. 2020; George et al. 2020; Zou et al. 2020). Eggshell has been coated with many photocatalytic materials for enhanced water treatment such as with TiO_2 (Dzinun et al. 2022), BiOBr (Deng and Guan 2013), ZnO (Elsayed et al. 2021), Cu/Fe_3O_4 (Nasrollahzadeh et al. 2016), Bi_2O_3 (Li et al. 2018) and so on. Several studies proved that CaO can be obtained from eggshell to be used as a photocatalytic material (Sree et al. 2020; Eskikaya et al. 2022).

The aim of this work is to prepare CuO-coated CaO material (ES@CuO, obtained from eggshell waste) for the photocatalytic removal of basic fuchsin (BF) under visible light irradiation. The optimization of the synthetic parameters, including CuO ratio and calcination temperature, was carried out to maximize the photocatalytic performance. The effect of operational factors such as pH solution, photocatalyst dosage, contact time, initial dye concentration, and temperature was investigated to determine the optimal conditions. The performance of ES@CuO in dark and under light irradiation was compared and discussed. The regeneration and recycling of the various ES@CuO were studied to determine the long-term stability of the material.

Materials and methods

Basic fuchsin (BF) and copper (II) chloride dihydrate ($CuCl_2, 2H_2O$) used in this study were obtained from Sigma-Aldrich-Fluka (Saint-Quentin, Fallavier, France). Chicken eggshell waste was collected from a local restaurant in Souk Ahras province, Eastern Algeria. The pH adjustment of the solution was controlled by a pH Meter (HANNA HI98125). The dye used in this study is basic fuchsin (BF), also known as triaminotriphenylmethane ($C_{20}H_{20}ClN_3$).

Preparation of ES biomaterial

The collected eggshells were thoroughly washed with tap water to remove any surface contaminants. The clean shells were then boiled in distilled water for 15 min to remove all remaining bacteria and the inner membranes were manually separated. The membraneless biomaterial was then dried in an oven at 105 °C for 24 h. The recovered amount was crushed and sieved to obtain a fine and uniform powder, of which only particles with a size in the 100–250 nm range were used.

Preparation of ES@CuO photocatalyst

The ES@CuO photocatalysts were prepared at different percentages of CuO by the hydrothermal method, which consists in mixing a determinant quantity of ES with a 100 mL solution of copper (II) chloride dihydrate at different concentrations (1, 2, and 4 g/L). The mixtures were then placed under mechanical stirring for 24 h at room temperature, followed by filtration, and transferred to a muffle furnace, where calcination took place at different temperatures (600, 800 and 1000 °C) for 3 h at a rate of 12 °C/min. This step was carried out to obtain ES@CuO photocatalysts with different CuO final percentages (2.5%, 5%, and 10%).

Characterization

FTIR-ATR spectra were obtained on solid samples with a Bruker Vertex 70 spectrophotometer equipped with Harrick MVP2 ATR cell and DTGS detector (64 scan, 4 cm^{-1} resolution). FT-Raman spectra were obtained with the same instrument, equipped with the RAMII accessory and Ge detector, by exciting samples with Nd:YAG laser source (1064 nm), with resolution of 4 cm^{-1}. The morphology of both eggshells (ES) and the photocatalyst morphology and elemental analyses were evaluated by means of a scanning electron microscope operating with a field emission source (FESEM), model TESCAN S9000G (Overcoached, Germany) equipped with a Schottky type FEG source; resolution: 0.7 nm at 15 keV (in In-Beam SE mode) and equipped with EDS Oxford Ultim Max (operated with Aztec software 6.0). The sample was supported on metallic stabs with C tape and then coated with Cr by means of ion-sputtering technique to improve the conductivity of the materials. X-ray diffraction (XRD) data in the 10–90 range was collected with Cu Ka radiation using a Philips X'Pert X-ray diffractometer to determine the possible crystalline phase(s) present in the materials.

Photocatalytic experiments and kinetic models

The photocatalytic tests to evaluate the performance of ES@CuO materials were tested for the oxidation of basic fuchsin (BF) in a 250 mL beaker under visible light irradiation (LED bulb, 10 W). The pH of the solution was adjusted with 0.1 M HCl and 0.1 M NaOH. At fixed time intervals, 4 mL of the solution was taken, centrifuged, and measured using a UV–Vis spectrophotometer (JENWAY 7315) at 550 nm.

Results and discussion

Characterization

Figure 1 reports both FTIR-ATR and FT-Raman spectra of raw ES and ES@CuO$_{5\%}$ photocatalyst. The occurrence of several characteristic peaks of calcite was observed in the case of the raw ES sample, in particular typical carbonate modes at 1400 (ν_3), 1085 (ν_1), 875 (ν_2), 715 (ν_4) cm^{-1} (see section a in Fig. 1). In the Raman spectrum (see section b in Fig. 1), other diagnostic peak of calcite are evident, namely at 284 and 157 cm^{-1}, arising from external vibrations of the CO_3^{2-} groups (Gunasekaran et al. 2006). The broad peak observed in the 3600–3400 cm^{-1} region is related to the stretching vibration of the OH group of the adsorbed water molecules, whose bending mode is observed at ca. 1650 cm^{-1}. Calcium oxide does not possess any Raman-active modes and IR-active modes are expected in far IR
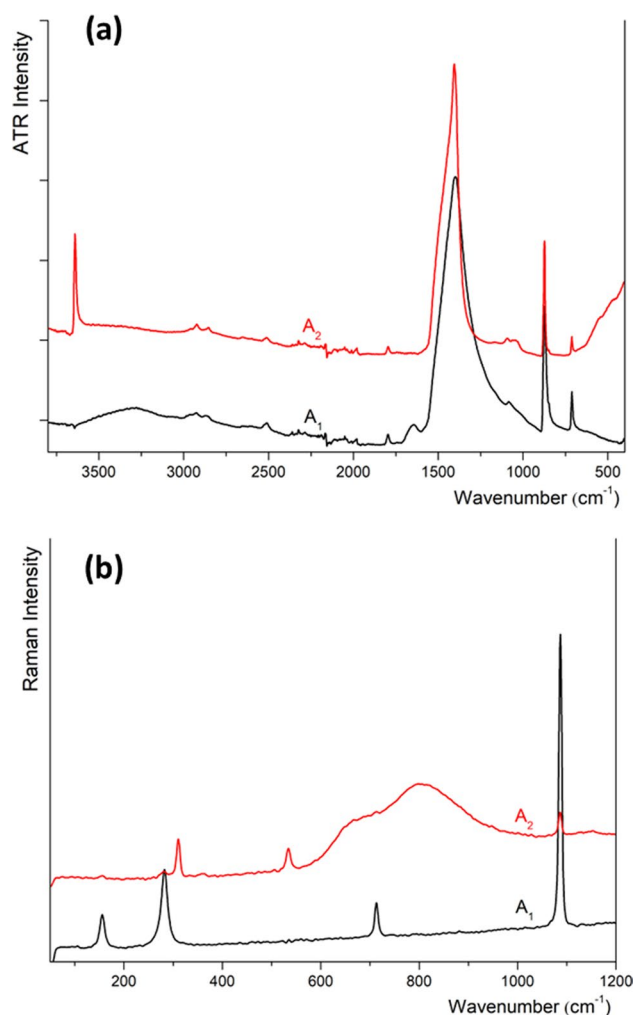

Fig. 1 **a**: FTIR-ATR and **b** FT-Raman spectra of (A$_1$) Raw ES and (A$_2$): ES@CuO$_{5\%}$

region (not observed) (Schmid and Dariz 2015), but some signals are observed in both Raman and ATR spectra of ES@CuO$_{5\%}$ photocatalyst, due to inevitable traces of Ca(OH)$_2$ and CaCO$_3$ formed in this highly reactive material. In fact, in the FTIR-ATR spectrum (see section a in Fig. 1) we observe a sharp peak at 3640 cm^{-1}, ascribable to the stretching mode of OH groups belonging to surface water, and some characteristic bands of carbonate groups (in the form of a broad and intense absorption in the 1600–1200 cm^{-1} spectral range and as tiny band(s) in the 1150–1000 cm^{-1} range). In the Raman spectrum of ES@CuO$_{5\%}$ the occurrence of a signal at 310 cm^{-1} confirms the formation of CuO (Hagemann et al. 1990).

Figure 2a refers to the morphological characterization carried out by FESEM. It is evident that the raw ES exhibits a hard and sharp surface structure, with no protrusions or noticeable pores, which reduces their adsorption ability. However, calcined ES (Fig. 2b) and calcined
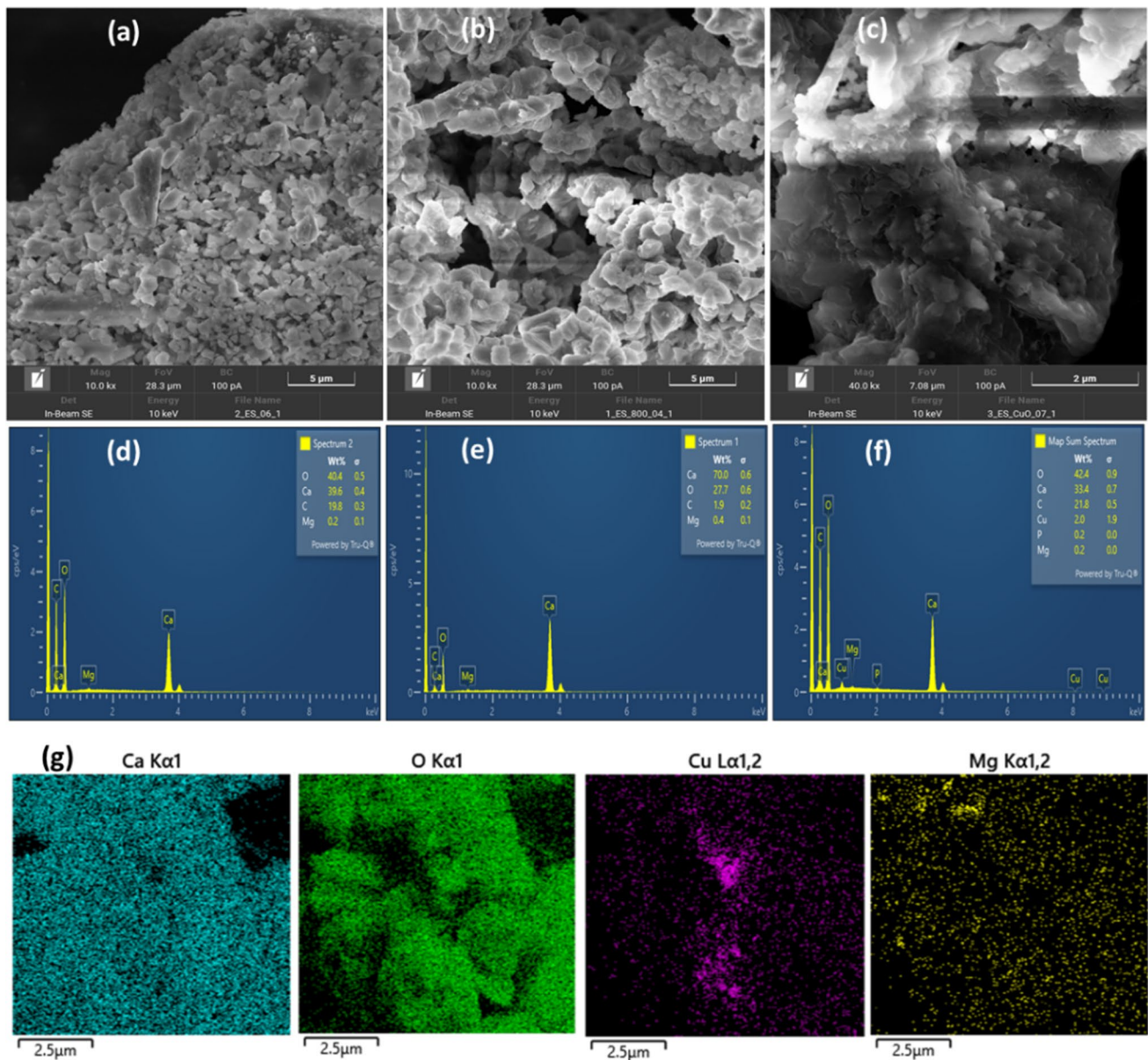
Fig. 2 SEM images of **a** raw ES, **b** ES_800 and **c** ES@CuO$_{5\%}$_800. EDS spectra of **d** ES, **e** ES_800 and **f** ES@CuO$_{5\%}$800. **g** EDS elemental mapping of ES@CuO$_{5\%}$800

ES coated with CuO particles (Fig. 2c), a new layer with heterogeneous morphology and irregular distribution was formed on their surface. Due to the well-integrated CuO particles, the photocatalyst exhibits a high porosity. It is further aggravated through voids and holes ranging from 0.1 to 5 μm in size.

EDS spectra show the presence of Ca, C, O and Mg (Fig. 2d, e, f). The content of Ca increases from 40 to 70% after calcination at 800 °C which attributed to conversion of CaCO$_3$ (40% Ca) to CaO (70%). In the case of ES@CuO$_{5\%}$, Cu element appeared with ratio of 2%. The distribution of elements including Ca, Cu, O and Mg is shown the EDS

elemental mapping images (Fig. 2g). CuO is well dispersed on the surface of CaO, allowing good efficiency.

Figure 3 shows the XRD pattern of the raw ES and ES@CuO$_{5\%}$ photcatalysts calcined at 600, 800, and 1000 °C. The XRD pattern indicates the presence of a CaCO$_3$ rhombohedral phase in raw ES and ES@CuO$_{5\%}$ catalyst calcined at 600 °C as well, with the highest diffraction peak at 2θ = 29°, which is in good agreement with the reported standards values. The intensity of this peak is higher in ES@CuO$_{5\%}$ calcined at 600 °C and might be due to the removal of grain boundary, leading to an enhanced crystal size. At higher calcination temperatures (800 and 1000 °C, respectively),
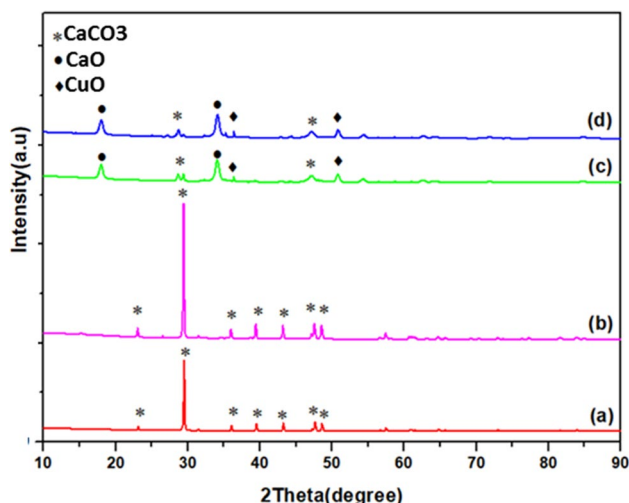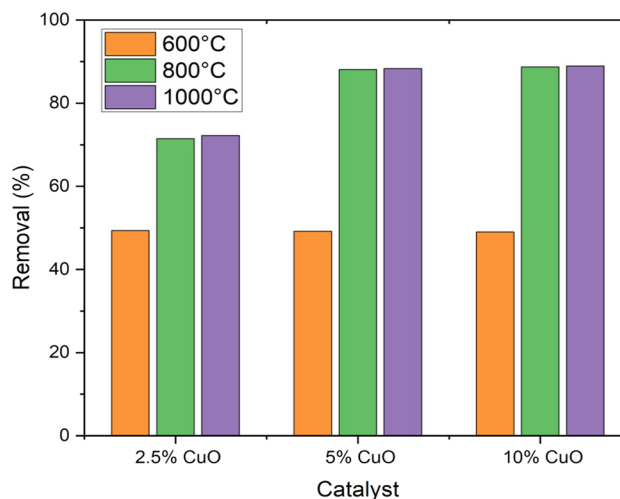
Fig. 3 XRD analysis of **a** raw ES, **b** ES@CuO$_{5\%}$ 600, **c** ES@CuO$_{5\%}$ 800, and **d** ES@CuO$_{5\%}$ 1000

Fig. 4 The effect of CuO percentage and calcination temperature on the efficiency of BF degradation ([ES@CuO] = 50 mg/L; C$_0$ = 100 mg/L; t = 30 min; T = 25 °C; pH = 6,8)

both CuO and CaO diffraction peaks are evident. The transformation of the rhombohedral form (CaCO$_3$) into a face centered cubic form (CaO) requires higher calcination temperature to allow the decomposition of CaCO$_3$ and the crystallization processes to form CaO (Risso et al. 2018). It was reported in the literature that the transformation of CaCO$_3$ into CaO is optimal at calcination temperature of ca. 900 °C (Tangboriboon et al. 2012). At a calcination temperature of 600 °C, characteristic peaks of CuO are absent and this feature could be due to the low crystallite size. It is important to mention that the ratio of CuO in CaO is only 5%, and if the crystallinity is very low, peaks can be hardly detected. The increase of temperature pushes the crystallite size due to the boosted atom diffusion which enhances the generation of crystal nucleation phases. The raising of temperature leads to remove grain boundary, resulting in better crystallinity.

Photocatalytic tests

Effect of CuO ratio and calcination temperature

To evaluate the performance of different samples, photocatalytic experiments for the oxidation of Basic Fuchsin (BF) were performed with composites at various CuO percentages (2.5%, 5%, and 10%), previously calcined at 600 °C, 800 °C, and 1000 °C and the results are reported in Fig. 4. It can be seen that ES@CuO$_{5\%}$ and ES@CuO$_{10\%}$ exhibit higher photocatalytic oxidation as compared to ES@CuO$_{2.5\%}$. Meanwhile, ES@CuO$_{5\%}$ and ES@CuO$_{10\%}$ exhibit similar performance. In addition, samples calcined at 800 and 1000 °C are more effecient for the oxidation of BF dye and this might bedue to the formation of CaO and CuO oxides at these temperature values, in opposition to lower

calcination temperature 600 °C. The oxidation rates were found to be 88.11% and 88.33% using ES@CuO$_{5\%}$800 °C and ES@CuO$_{5\%}$1000 °C, respectively. Due to the efficiency and less energy and chemical consumption, ES@CuO$_{5\%}$ sample was selected as optimal photocatalyst to carry on the next experiments.

Effect of operating parameters on photocatalytic oxidation

Studying the effect of pH solution on the photocatalytic process is an important step in understanding the impact of degradation experiments in a complex environment. Photocatalytic tests were conducted under different pH values ranging from 2 to 12 under visible light irradiation for 30 min, and the obtained results are shown in Fig. 5a. Overall, the performance of dye removal was better at pH 6.8, and similar BF removal are observed at basic pH values, while at acidic pH values the removal decreases by more than the half. During the photocatalytic activity, the adsorption or surface interaction is a crucial factor to get effective radical oxidation due to the short half time of photogenerated reactive oxygen species (ROS) (Nouacer and Djellabi 2023; Radji et al. 2024). The pH can affect the charge of the photocatalyst surface by protonation at acidic medium and deprotonation at basic pH, which make the surface positively or negatively charged, respectively. Since BF is a cationic dye, absorption is favored on negatively charged surface.

The effect of ES@CuO$_{5\%}$ photocatalyst mass on BF degradation was studied in the range of 25–150 mg/L (Fig. 5b). As the catalyst mass increases, the oxidation rate increases, and total removal of the dye is observed for mass values greater than 75 mg/L. The increase in the performance with the increase of photocatalyst mass is related to the higher
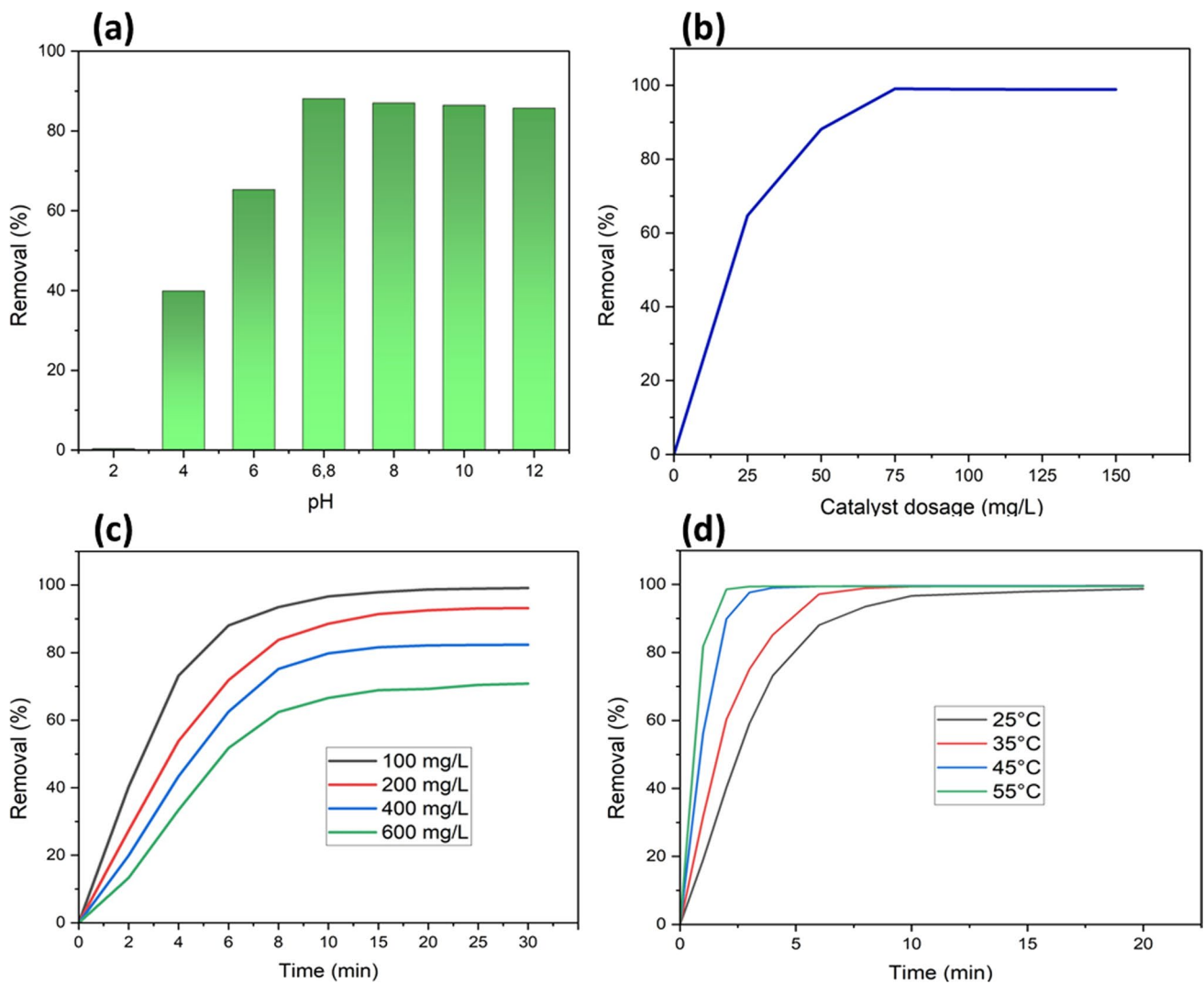
Fig. 5 a Effect of solution pH on the degradation rate of BF dye ([ES@CuO$_{5\%}$] = 50 mg/L; C$_0$ = 100 mg/L; t = 30 min; T = 25 °C). **b**: Effect of photocatalyst dosage on the degradation rate of BF dye (C$_0$ = 100 mg/L; t = 30 min; T = 25 °C; pH = 6.8). **c**: Effect of initial dye concentration on BF degradation efficiency ([ES@CuO$_{5\%}$] = 75 mg/L; t = 30 min; T = 25 °C; pH = 6.8). **d** Effect of temperature on the degradation rate of BF dye ([ES@CuO$_{5\%}$] = 75 mg/L; C$_0$ = 100 mg/L; t = 20 min; pH = 6.8)

number of available active sites and so an high yield of photogenerated oxidative ROS. In a normal scenario, an optimum mass of photocatalyst could be the maximum amount when the surface is well irradiated to generate ROS before reaching the phenomenon of screen effect (Ernawati et al. 2021). The optimization of the photocatalyst mass depends on several factors including the size and density of the photocatalyst, irradiation intensity, photoreactor configuration and stirring conditions.

The effect of BF concentration on the oxidation rate was carried out at various values including 100, 200, 400, and 600 mg/L, at neutral pH and room temperature. The obtained results are presented in Fig. 5c. ES@CuO$_{5\%}$ proved to be effective material for the removal of BF under light irradiation, even at concentrations relatively high compared to real

conditions.. The increase of BF concentration from 100 to 600 mg/L reduced the oxidation rate only with 30%, suggesting a superior performance of ES@CuO$_{5\%}$. The higher concentration might delay the oxidation by photogenerated ROS due to the accumulation of surface blockage and screen effect (Yang et al. 2021).

The effect of temperature on the photocatalytic oxidation of BF using ES@CuO$_{5\%}$ was studied within the range 25–55 °C and the results are shown in Fig. 5d. It was found that the removal rates are the same within 20 min, while the kinetics is faster whit increasing temperature. At 55 °C, a total removal of BF dye was observed within only2 min. In photocatalytic reaction, the effect of temperature is basically related to the enhanced mass transfer, rather than the photocatalytic action itself. The physical adsorption of dye

species on the surface of the photocatalyst is promoted by heat, allowing quick radical interaction and so oxidation.
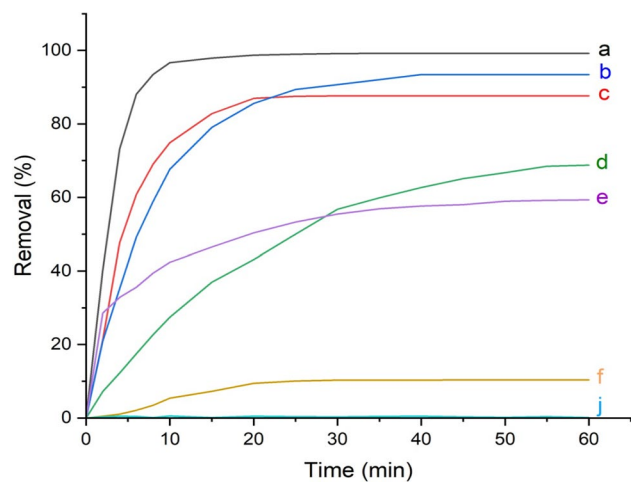
Photocatalyst reuse

The recyclability of catalysts is a crucial factor at large scale from the economic and sustainability points of view (Djellabi et al. 2021). The deactivation can take place through two main processes: chemical degradation of the catalyst itself or deposition of chemical species on the surface. After each treatment, the photocatalyst was filtered and separated from the treated water, washed three times with distilled water, and then dried in an oven at 60 °C. Figure 6 shows that in the case of the unwashed catalyst, the BF removal efficiency dropped from 99.17% to about 54.72% after five cycles and 37.34% after six cycles of use. On the other hand, the efficiency of the washed catalyst decreased from 99.17 to 60.53% after five cycles and down to 48.53% after the sixth cycle. It can be deduced that the treatment of the catalyst after each use might increase the long time of the photocatalyst as the by-products can be removed. Even though, there was a reduction in the efficiency which could be due to leaching of CuO particles leading to a partial change in the characteristic of the photocatalyst.

Comparison between photocatalysis and adsorption

To evaluate the contribution of CaO and CuO in ES@CuO$_{5\%}$ composite photocatalyst, adsorption and photocatalytic studies using bare CaO (obtained from ES), bare CuO and ES@CuO$_{5\%}$ were carried out under the same conditions. The obtained results are shown in Fig. 7. Firstly, it can be noticed that bare CaO showed excellent adsorption and photocatalytic activity. Under light irradiation, the removal of
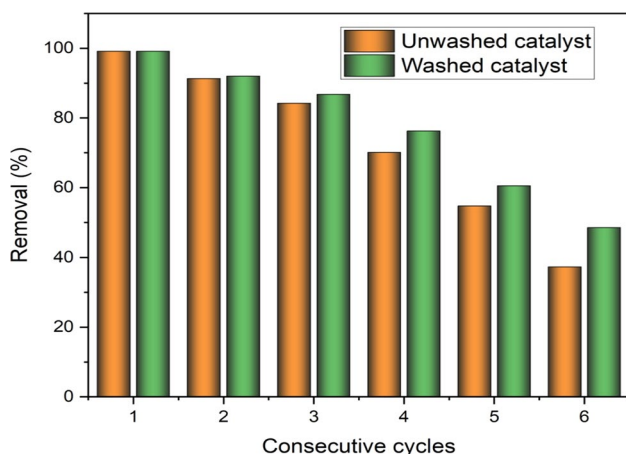

Fig. 6 Consecutive cycles of ES@CuO$_{5\%}$ catalyst for BF degradation with and without washing ([ES@CuO$_{5\%}$] = 75 mg/L; C_0 = 100 mg/L; t = 30 min; T = 25 °C; pH = 6,8)

Fig. 7 BF removal efficiency as a function of time using **a** ES@CuO$_{5\%}$ in light conditions, **b** Calcined ES in light conditions, **c** ES@CuO$_{5\%}$ photocatalyst in dark conditions, **d** Calcined ES in dark conditions, **e** CuO in light conditions, **f** CuO in dark conditions, and **j** light, ([material]: 75 mg/L; C_0 = 100 mg/L; T = 25 °C; pH = 6,8)

the dye was found to be around 90% within the first 30 min, against 57% without light irradiation. This proves the high efficiency of this low cost material even without modification. ES is rich of calcium carbonate, around 94% (Sree et al. 2020), which can be converted by thermal heating into photoactive CaO. As above discussed, the heat treatment is very important to obtain a highly adsorptive and photoactive material. Solid CaO is made of an array of Ca^{2+}, and O^{2-}, and it exhibits a wide band gap which is not able to produce ROS under visible light via the photoexcitation process (Bolorizadeh et al. 2004). The oxidation of dye by CaO under visible light could be driven by photosensitizing effect, wherein dye molecules absorb visible light and transfer the obtained energy to CaO (Peralta et al. 2018). In this study, the adsorption capacity of ES@CuO$_{5\%}$ photocatalyst was studied in dark conditions and compared to the photodegradation capacity of ES@CuO$_{5\%}$ and light photolysis capacity, as shown in Fig. 7. It can be observed that the light has no effect on the degradation of the dye. The adsorption capacity of ES@CuO$_{5\%}$ in dark is around 87%, but under light condition the removal efficiency is 96.63% in 10 min and 99% in 30 min. These results demonstrate the role of CuO in dye degradation. The synergistic effects of adsorption and photocatalytic action can be behind the fast removal of BF dye. This synergism is known as Adsorb and Shuttle process (Djellabi et al. 2020; Mergbi et al. 2023). In this process, the adsorbing area concentrates the amount of dye pollutant nearby the photoactive area, favoring the oxidation process. In general, the use plain photocatalysts suffers from the mass transfer, and in addition, a high adsorption of pollutant on the surface of plain photocatalysts might limit the photocatalytic generation of ROS due to the screen effect (Nouacer
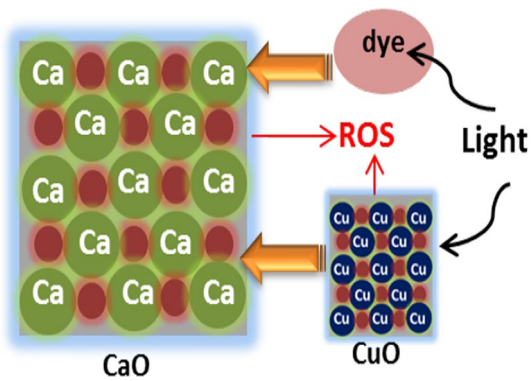
Fig. 8 Plausible mechanistic pathways for the removal of dye by ES@CuO composite under visible light

and Djellabi 2023). Therefore,, the combination of adsorptive materials and photoactive nanoparticles is regarded as one of the best option to enhance the photocatalytic kinetics for the removal of pollutants from water (Djellabi et al. 2021). On top to the Adsorb and Shuttle process, the combination of CaO and CuO, followed by calcination, led to the formation of optimized heterojunction system which allows the absorption of visible light and boosts the separation of photogenerated charges. CaO is known for its wide band gap and low photocatalytic activity (Ikram et al. 2022), which requires structural and surface modification to enhance its performance. This study shows that bare CaO exhibits excellent photocatalytic activity under visible light which could be explained by the dye photosensitizing effect (Djellabi et al. 2017). In this process, the dye absorbs the light, then after excitation, it transfers energy to CaO, leading to photogenerate ROS (Koh et al. 2017). In addition, CuO is recognized as effective photocatalyst under visible light itself and also it can catalyze the photosensistizing effect (Raizada et al. 2020) which in turn enhances the photogeneration of ROS by the ES@CuO composite. The possible mechanisms of dye degradation by ES@CuO are simplified in Fig. 8.

It should be noted that ES@CuO composite proves to be an effective photocatalyst for the removal of BF under visible light irradiation. The total removal of 100 mg/L of BF can be achieved within less than 30 min under irradiation using 0.075 g/L of the photocatalyst. This is considered as relatively fast compared to most reported photocatalysts. For example, Zhang et al. (2021) reported that the removal of 30 mg/L using 0.2 g/L of 5%-Eu-doped ZIF-8(Eu)@Mc-TiO2 requires 1 h under UV light irradiation. In another study, 0.6 g/L of $Ce(MoO_4)_2$ was used to remove BF at 3.10^4 M (~ 97 mg/L) under solar light with 100 min. Most of other reported materials showed lower performance compared to ES@CuO composite. On top of that, ES@CuO is very cheap which could be obtained from available food waste including the incorporation of 5% of CuO and thermal treatment.

Conclusion

The finding of this investigation proves the excellent performance of CuO coated ES-based CaO for the phoyocatalytic oxidation of BF dye under visible light. The transformation of ES-based $CaCO_3$ into CaO takes place at calcination temperature ≥ 800 °C. The results of photocatalytic oxidation of BF under visible light was found to be superior using samples with CuO ratios of 5 or 10%, while it was weaker at lower CuO ratio (2.5%). To summarize, $ES@CuO_{5\%}$ calcined at 800 °C was considered as the most effective catalyst that requires the lowest chemicals and energy consumption. $ES@CuO_{5\%}$ proves superior removal of BF under visible light irradiation at concentration ranging from 100 to 600 mg/L using 0.75 mg/L of photocatalyst. It was found that the removal is relatively fast compared to other common systems. $ES@CuO_{5\%}$ combines both physical adsorption and radical oxidation by photogenerated ROS. $ES@CuO_{5\%}$ showed excellent recycling ability which suggests its chemical and physical stability. Overall, the design of photocatalysts from wastes is regarded as sustainable and green technology that fits well with the aspects of circular economy and sustainable devolvement. This study shows significant pros in terms of low-cost valuable products and valorization of food wastes for environmental remediation.

Author contributions Atef Ali Ahmed: Methodology, Investigation, Formal analysis and Writing—original draft; Yamina Berredjem & Zhour Hattab: Supervision, Project administration, Conceptualization, writing and review, Alessia Giordana & Giuseppina Cerrato: Investigation, review and validation; Ridha Djellabi: Supervision, Writing—review & editing.

Declarations

Conflict of interest The authors declare that they have no known competing financial interests or personal relationships that could have appeared to influence the work reported in this paper.

Ethical approval Not applicable.

Consent to participate The study does not involve any human participants, human data, or human tissues.

Consent for publication All authors have read and approved the final manuscript to be published.

References

Aboagye D, Djellabi R, Medina F, Contreras S (2023) Radical-mediated photocatalysis for lignocellulosic biomass conversion into value-added chemicals and hydrogen: facts, opportunities and challenges. Angew Chem Int Ed 62:e202301909

Ambaye TG, Djellabi R, Vaccari M, Prasad S, Aminabhavi T, Rtimi S (2023) Emerging technologies and sustainable strategies for municipal solid waste valorization: challenges of circular economy implementation. J Clean Prod. https://doi.org/10.1016/j.jclepro.2023.138708

Andhalkar VV, Foong SY, Kee SH, Lam SS, Chan YH, Djellabi R, Bhubalan K, Medina F, Constantí M (2023) Integrated biorefinery design with techno-economic and life cycle assessment tools in polyhydroxyalkanoates processing. Macromol Mater Eng 308(11):2300100

Bolorizadeh MA, Sashin V, Kheifets A, Ford M (2004) Electronic band structure of calcium oxide. J Electron Spectrosc Relat Phenom 141(1):27–38

Cao S, Wu X, Zhu Y, Gupta R, Tan A, Wang Z, Jun Y-S, Singamaneni S (2020) Polydopamine/hydroxyapatite nanowire-based bilayered membrane for photothermal-driven membrane distillation. Journal of Materials Chemistry A 8(10):5147–5156

Carvalho J, Araújo J, Castro F (2011) Alternative low-cost adsorbent for water and wastewater decontamination derived from eggshell waste: an overview. Waste and Biomass Valorization 2:157–167

De Angelis G, Medeghini L, Conte AM, Mignardi S (2017) Recycling of eggshell waste into low-cost adsorbent for Ni removal from wastewater. J Clean Prod 164:1497–1506

Deng C, Guan H (2013) Fabrication of hollow inorganic fullerene-like BiOBr eggshells with highly efficient visible light photocatalytic activity. Mater Lett 107:119–122

Djellabi R, Ghorab MF, Sehili T (2017) Simultaneous removal of methylene blue and hexavalent chromium from water using TiO2/Fe (III)/H2O2/sunlight. CLEAN–Soil, Air, Water 45(6):1500379

Djellabi R, FouziGhorab M, Smara A, Bianchi CL, Cerrato G, Zhao X, Yang B (2020) Titania-Montmorillonite for the photocatalytic removal of contaminants from water: adsorb & shuttle process. Green materials for wastewater treatment. Springer, Cham, pp 291–319

Djellabi R, Giannantonio R, Falletta E, Bianchi CL (2021) SWOT analysis of photocatalytic materials towards large scale environmental remediation. Curr Opin Chem Eng 33:100696

Djellabi R, Aboagye D, Galloni MG, Andhalkar VV, Nouacer S, Nabgan W, Rtimi S, Constantí M, Cabello FM, Contreras S (2022) Combined conversion of lignocellulosic biomass into high-value products with ultrasonic cavitation and photocatalytic produced reactive oxygen species-A review. Bioresour Technol 368:128333

Dzinun H, Abd Khalid NH, Hairom NHH (2022) Photocatalytic performance of TiO2/Eggshell composite for wastewater treatment. Mater Today: Proc 65:3000–3006

Elsayed MS, Ahmed IA, Bader DM, Hassan AF (2021) Green synthesis of nano zinc oxide/nanohydroxyapatite composites using date palm pits extract and eggshells: adsorption and photocatalytic degradation of methylene blue. Nanomaterials 12(1):49

Ernawati L, Yusariarta AW, Laksono AD, Wahyuono RA, Widiyandari H, Rebeka R, Sitompul V (2021). Kinetic studies of methylene blue degradation using CaTiO3 photocatalyst from chicken eggshells. Journal of Physics: Conference Series, IOP Publishing

Eskikaya O, Gun M, Bouchareb R, Bilici Z, Dizge N, Ramaraj R, Balakrishnan D (2022) Photocatalytic activity of calcined chicken eggshells for Safranin and Reactive Red 180 decolorization. Chemosphere 304:135210

Galloni M, Sharif H, Grainca A, Haider MR, Djellabi R (2024) Magnetic adsorbents/photocatalysts for water purification: progress and challenges. Royal Society of Chemistry, London

George S, Mehta D, Saharan VK (2020) Application of hydroxyapatite and its modified forms as adsorbents for water defluoridation: an insight into process synthesis. Rev Chem Eng 36(3):369–400

Gunasekaran S, Anbalagan G, Pandi S (2006) Raman and infrared spectra of carbonates of calcite structure. J Raman Spectrosc 37(9):892–899

Hagemann H, Bill H, Walker E, François M (1990) Raman spectra of single crystal CuO. Solid State Commun 73(6):447–451

Ikram M, Khalid A, Shahzadi A, Haider A, Naz S, Naz M, Shahzadi I, Ul-Hamid A, Haider J, Nabgan W (2022) Enhanced photocatalytic degradation with sustainable CaO nanorods doped with Ce and cellulose nanocrystals: in silico molecular docking studies. ACS Omega 7(31):27503–27515

Koh PW, Hatta MHM, Ong ST, Yuliati L, Lee SL (2017) Photocatalytic degradation of photosensitizing and non-photosensitizing dyes over chromium doped titania photocatalysts under visible light. J Photochem Photobiol, A 332:215–223

Laca A, Laca A, Díaz M (2017) Eggshell waste as catalyst: A review. J Environ Manage 197:351–359

Li J, Ng DH, Ma R, Zuo M, Song P (2017) Eggshell membrane-derived MgFe2O4 for pharmaceutical antibiotics removal and recovery from water. Chem Eng Res Des 126:123–133

Li Y, Hui B, Gao L, Li F, Li J (2018) Facile one-pot synthesis of wood based bismuth molybdate nano-eggshells with efficient visible-light photocatalytic activity. Colloids Surf, A 556:284–290

Luo J, Huang W, Guo W, Ge R, Zhang Q, Fang F, Feng Q, Cao J, Wu Y (2020) Novel strategy to stimulate the food wastes anaerobic fermentation performance by eggshell wastes conditioning and the underlying mechanisms. Chem Eng J 398:125560

Mandado M, Blockhuys F, Van Alsenoy C (2006) On the applicability of QTAIM, Hirshfeld and Mulliken delocalisation indices as a measure of proton spin–spin coupling in aromatic compounds. Chem Phys Lett 430(4–6):454–458

Mergbi M, Aboagye D, Contreras S, Amor HB, Medina F, Djellabi R (2023) Fast g-C3N4 sonocoated activated carbon for enhanced solar photocatalytic oxidation of organic pollutants through Adsorb & Shuttle process. Ultrason Sonochem 99:106550

Nasrollahzadeh M, Sajadi SM, Hatamifard A (2016) Waste chicken eggshell as a natural valuable resource and environmentally benign support for biosynthesis of catalytically active Cu/eggshell, Fe3O4/eggshell and Cu/Fe3O4/eggshell nanocomposites. Appl Catal B 191:209–227

Nayak A, Bhushan B (2019) An overview of the recent trends on the waste valorization techniques for food wastes. J Environ Manag 233:352–370

Nouacer S, Djellabi R (2023) Easy-handling semi-floating TiO2-based aerogel for solar photocatalytic water depollution. Environ Sci Pollut Res 30(9):22388–22395

Ononiwu NH, Akinlabi ET (2020) Effects of ball milling on particle size distribution and microstructure of eggshells for applications in metal matrix composites. Mater Today: Proc 26:1049–1053

Peralta MLR, Sánchez-Cantú M, Puente-López E, Rubio-Rosas E, Tzompantzi F (2018) Evaluation of calcium oxide in rhodamine 6G photodegradation. Catal Today 305:75–81

Radji G, Houhou I, Hiri A, Djellabi R, Bettahar N (2024) Textural properties and adsorption behaviour of recyclable Ni–Al layered double hydroxides for Congo red and Alizarin red S dyes removal in single and binary systems. Process Saf Environ Prot 184:1251–1270. https://doi.org/10.1016/j.psep.2024.02.023

Raizada P, Sudhaik A, Patial S, Hasija V, Khan AAP, Singh P, Gautam S, Kaur M, Nguyen V-H (2020) Engineering nanostructures of CuO-based photocatalysts for water treatment: current progress and future challenges. Arab J Chem 13(11):8424–8457

Risso R, Ferraz P, Meireles S, Fonseca I, Vital J (2018) Highly active Cao catalysts from waste shells of egg, oyster and clam for biodiesel production. Appl Catal A 567:56–64

Schmid T, Dariz P (2015) Shedding light onto the spectra of lime: Raman and luminescence bands of CaO, Ca (OH) 2 and CaCO3. J Raman Spectrosc 46(1):141–146

Singh A, Kelkar N, Natarajan K, Selvaraj S (2021) Review on the extraction of calcium supplements from eggshells to combat waste generation and chronic calcium deficiency. Environ Sci Pollut Res 28:46985–46998

Sree GV, Nagaraaj P, Kalanidhi K, Aswathy C, Rajasekaran P (2020) Calcium oxide a sustainable photocatalyst derived from eggshell for efficient photo-degradation of organic pollutants. J Clean Prod 270:122294

Tangboriboon N, Kunanuruksapong R, Sirivat A (2012) Preparation and properties of calcium oxide from eggshells via calcination. Mater Sci-Pol 30:313–322

Vickers NJ (2017) Animal communication: when i'm calling you, will you answer too? Curr Biol 27(14):R713–R715

Waheed M, Butt MS, Shehzad A, Adzahan NM, Shabbir MA, Suleria HAR, Aadil RM (2019) Eggshell calcium: a cheap alternative to expensive supplements. Trends Food Sci Technol 91:219–230

Yang Y, Ali N, Khan A, Khan S, Khan S, Khan H, Xiaoqi S, Ahmad W, Uddin S, Ali N (2021) Chitosan-capped ternary metal selenide nanocatalysts for efficient degradation of Congo red dye in sunlight irradiation. Int J Biol Macromol 167:169–181

Zaman T, Mostari M, Mahmood MAA, Rahman MS (2018) Evolution and characterization of eggshell as a potential candidate of raw material. Cerâmica 64:236–241

Zhai H, Liu F, Huang Y, Yang Q, Tian C, Zhou W (2022) Preparation of peanut shell-like calcium carbonate from biowaste chicken eggshell and its application for aqueous Victoria Blue B removal. Microporous Mesoporous Mater 329:111549

Zhang W, Liu H, Liu Z, An Y, Zhong Y, Hu Z, Li S, Chen Z, Wang S, Sheng X (2021) Eu-doped zeolitic imidazolate framework-8 modified mixed-crystal TiO2 for efficient removal of basic fuchsin from effluent. Materials 14(23):7265

Zou R, Xu T, Lei X, Wu Q, Xue S (2020) Novel and efficient red phosphorus/hollow hydroxyapatite microsphere photocatalyst for fast removal of antibiotic pollutants. J Phys Chem Solids 139:109353

Authors and Affiliations

A. Ali Ahmed[1,2] · Z. Hattab[2] · Y. Berredjem[2] · A. Giordana[3] · G. Cerrato[3] · R. Djellabi[4]

✉ R. Djellabi
ridha.djellabi@urv.cat

[1] Laboratory of Physics Matter and Radiation, University Mohammed Cherif Messaadia, Souk-Ahras, Algeria

[2] Laboratory of Water Treatment and Valorization of Industrial Wastes, Department of Chemistry, University Badji Mokhtar, B.P.12, 23000 Annaba, Algeria

[3] Department of Chemistry, University of Turin, Via Pietro Giuria 7, 10125 Turin, Italy

[4] Department of Chemical Engineering, Universitat Rovira i Virgili, 43007 Tarragona, Spain